Wiley
International Journal of Energy Research
Volume 2024, Article ID 6107765, 13 pages
https://doi.org/10.1155/2024/6107765

WILEY

Research Article

Continuous Monitoring of Water Levels for Industrial Boilers Using Single-Stage Object Recognition YOLOv5

Jongwon Kim,[1] **Minjun Kwon**,[2,3] **Byeongchan So**,[1] **Sewon Kim**,[2] **and Hongyun So**[1,3]

[1]*Department of Medical and Digital Engineering, Hanyang University, Seoul 04763, Republic of Korea*
[2]*Korea Institute of Industrial Technology (KITECH), Cheonan, Chungnam 31056, Republic of Korea*
[3]*Department of Mechanical Engineering, Hanyang University, Seoul 04763, Republic of Korea*

Correspondence should be addressed to Hongyun So; hyso@hanyang.ac.kr

Received 13 February 2024; Revised 26 July 2024; Accepted 6 August 2024

Academic Editor: Payman Jalali

This paper presents a measurement method that utilizes object recognition technology for continuous and quantitative real-time monitoring of water levels in industrial boilers. Real-time videos of water levels were monitored using a small camera, and the YOLO algorithm, a single-stage detector, was employed to use the bounding boxes of detected objects within the video as variables, directly measuring the length ratio for each frame. The method demonstrated a high level of accuracy in water-level measurement, with an average of 99.02%, and a stable performance, with a fluctuation of 0.13% in continuous measurements. Consequently, the proposed measurement method proves feasible for quantifying continuous water levels in industrial inspection systems even in low-resource environments. These results demonstrate a new mechanism for monitoring technology, without requiring text detection, showing the potential for improving efficiency in complex boiler systems and the feasibility of reliable water-level measurement and control.

1. Introduction

Recent advancements in computer vision technology are providing substantial solutions across diverse industrial sectors. These technologies have been successfully applied to crop identification in agriculture [1, 2, 3], structural defect detection in construction [4, 5, 6], and remote tracking detection in drone systems [7], thereby enhancing overall efficiency. In future industrial systems that emphasize minimal labor and high efficiency, object recognition technology is increasingly valued. Its significance is particularly evident in fields that demand continuous and precise monitoring and control of various factors, such as industrial boilers [8]. Industrial boilers are commonly used to provide heat in a range of industries, including petrochemicals, food processing, pulp and paper, and power generation. To ensure the safe and efficient operation of boiler systems, it is essential to monitor and control various operating conditions precisely. One critical variable that directly affects the safety and efficiency of a boiler is the water level. According to the first law of thermodynamics, the supply heat required for steam generation decreases as the amount of water inside the boiler decreases, leading to improved boiler efficiency. However, if the water level in the boiler becomes too low, significant damage owing to boiler overheating can occur in the furnace tube [9]. Maintaining the internal water level within a safe range and quantifying it in real-time are important challenges for improving the efficiency of boiler systems.

As shown in Figures 1(a) and 1(b), the management of water levels in industrial boilers typically involves the use of conductivity level probes (also referred to as level switches). This method defines only the upper and lower limits through the level probes, allowing users to visually check if the water level is within the safety range using a water-level gauge. In the event that the water level exceeds the safety range, the conductivity level probes signal the activation or stoppage of the water pump. However, this current method of water level management makes it impossible to continuously quantify changing water levels in real-time.

To solve this problem, it is important to continuously detect and quantify the water level using real-time video

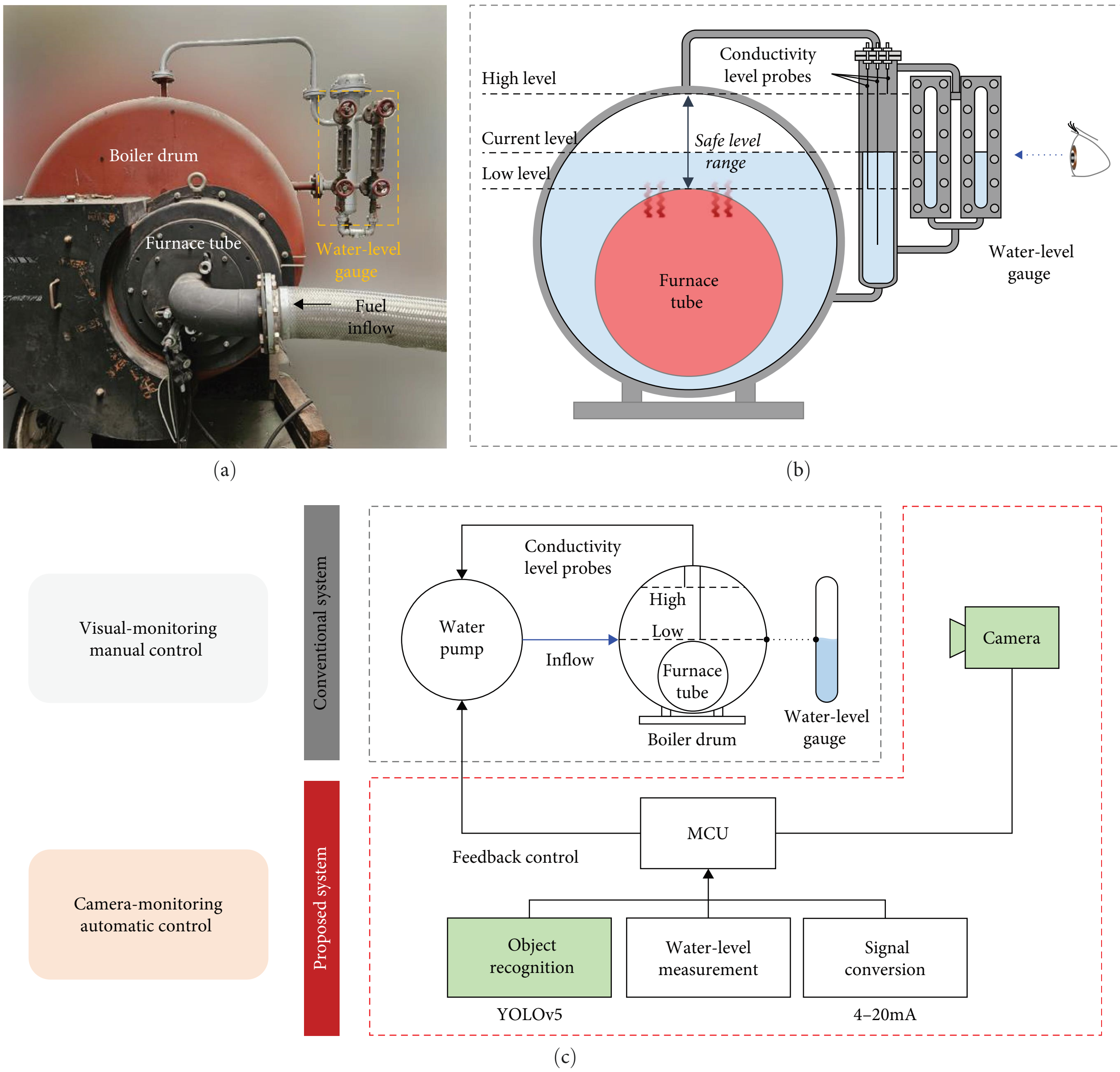

Figure 1: Overview of industrial boiler water-level management system: (a) industrial boiler and water-level gauge, (b) cross-sectional diagram, and (c) schematic diagram of the proposed water-level management system including object recognition technology.

information from the level gauge while maintaining the design elements of the existing boiler system.

In recent times, there have been several attempts to employ object recognition technology for measuring water levels [10, 11, 12, 13]. The application scenarios of the reported object recognition algorithms primarily involve detecting the position of the level gauge, the numbers on the scale, and the liquid-level line within the image. In particular, to read numbers at the water level involve extensive image-processing operations for number recognition [10, 11], and rely on the detection of the location information of the necessary parts within the image using a two-stage detector-based object recognition technique [12, 13]. This technique typically involves first generating candidate regions in which an object might be present, and then detecting the position and class of the object, which is primarily used for tasks that demand precise detection. While recognizing the numbers on the scale is an effective way to read the accurate water-level state, in the case of industrial boiler-level gauges, models without numeric scales are predominantly used. This may render these methods unsuitable for generalization. Moreover, measurement techniques that require extra image processing through object recognition, followed by complex computational structures, may not be cost-effective for real-time feedback control processing of water pumps in low-spec environments.

In this paper, a system for detecting water levels based on vision is proposed, as shown in Figure 1(c). This system uses object recognition technology to directly measure the water level without requiring text or number detection. The size of

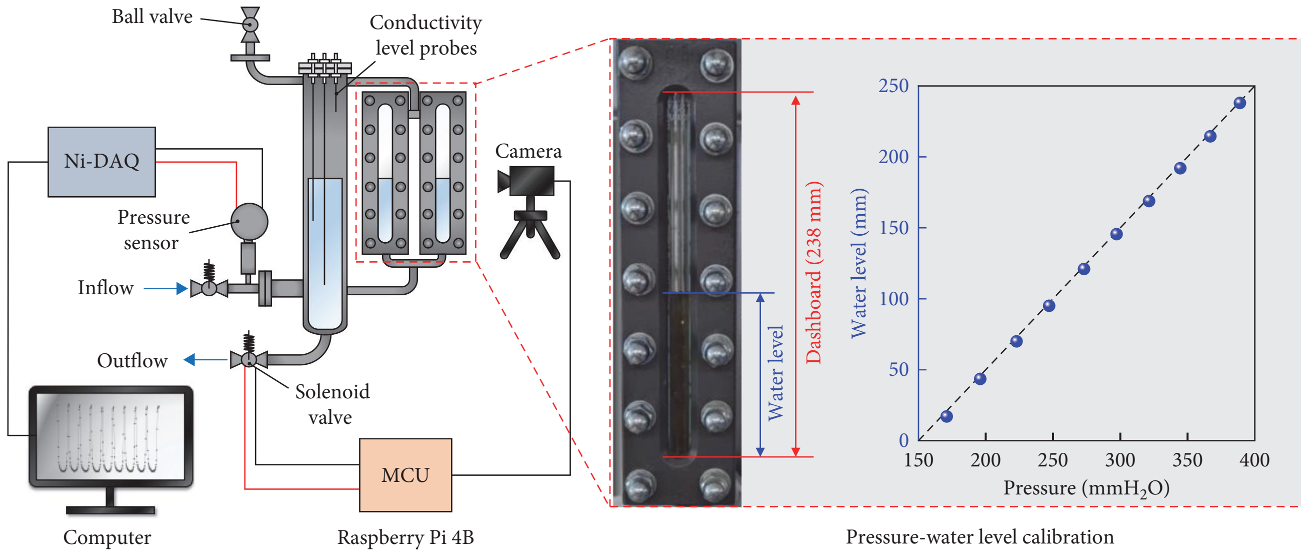

Figure 2: Schematic of the experimental setup for acquiring image data and evaluating water-level measurement performance.

extracted objects is used as variables. The system incorporates the single-stage algorithm YOLOv5 and a microcontroller unit (MCU), offering the advantage of a rapid response time [14]. First, data was collected to train the object recognition model. The detection performance of the trained models was then evaluated using performance metrics. Subsequently, by using well-trained models, we measured the water level and assessed the measurement performance by comparing it with the ground-truth values. Finally, the feasibility of using the proposed measurement method in industrial boilers was validated by evaluating the differences in the continuous water-level measurement performance based on the object detection performance at various water levels. This study aims to overcome the limitations of current systems that impede the enhancement of energy efficiency by ensuring consistent maintenance of the drum-level. Additionally, an effective continuous water-level measurement method was developed within the safe operational range of boilers, and the new potential applications of object recognition techniques were validated.

2. Materials and Methods

2.1. Experimental Design and Preparation. As shown in Figure 2, to train and evaluate the water-level detection model, an experimental setup was assembled using a water-level gauge (MAXOS®-DIN 7081), a pressure sensor (VPRNP-A6-500 mmH_2O), and an MCU (Raspberry Pi 4B). The water supply and discharge were controlled through two solenoid valves integrated with the water-level gauge. The state of the dashboard was recorded through a camera (used for dataset collection: Galaxy S23, object detection: Logitech®-C270). Pressure signals were obtained using a pressure sensor to validate the accuracy of the water-level measurement in the object detection model. The suitability of the pressure-signal performance evaluation is illustrated in Figure 2. A ruler was attached to the dashboard, and the water level was adjusted. The values on the ruler were compared with the pressure values corresponding to the height of the water supplied to the water-level gauge. The internal environment of the water-level gauge was maintained at atmospheric pressure. The linear results demonstrate the suitability of the pressure signal for evaluating the water-level measurement performance of the model.

2.2. Hardware Configuration. The YOLOv5 network-based model was trained and tested in a Colab server environment (Intel (R) Xeon (R) CPU @ 2.30 GHz (Dual-Core), NVIDIA TESLA T4, 8GB RAM). Additional model detection was performed on a Raspberry Pi 4B environment (Raspbian-64-bit OS). The experimental code was written in Python 3.9.2 and PyTorch 2.0.1.

2.3. Model Training. To train the YOLOv5 model, it is necessary to have images with bounding boxes in the Darknet format. For this purpose, Roboflow, a widely recognized web-based dataset-processing tool, was employed [15, 16, 17, 18]. The YOLO series is commonly employed for identifying classes and presence within images or videos, or for object extraction for subsequent processes, due to its fast response time and simple network structure [2, 3, 19]. To acquire variable water-level images, the water supply and drainage processes were repeated, and the water-level gauge was recorded on a video. Subsequently, 259 images were selected by splitting the frames at 1-s intervals (Figure 3). For the selected images, annotations and bounding boxes were manually added using the Roboflow Annotate annotation tool for two classes: "water" and "dashboard." The images were resized to 640×640 pixels. The processed images were then divided into three sets: training, validation, and test sets, in a ratio of 7 : 2 : 1. The model was trained using the training and validation sets, while the test set was used to evaluate the model's performance.

2.4. Mechanism of Detection and Measurement. Figure 4(a) shows the architecture of the YOLOv5 model used in this study. The model comprises three main components: backbone, neck, and head. The backbone is the fundamental

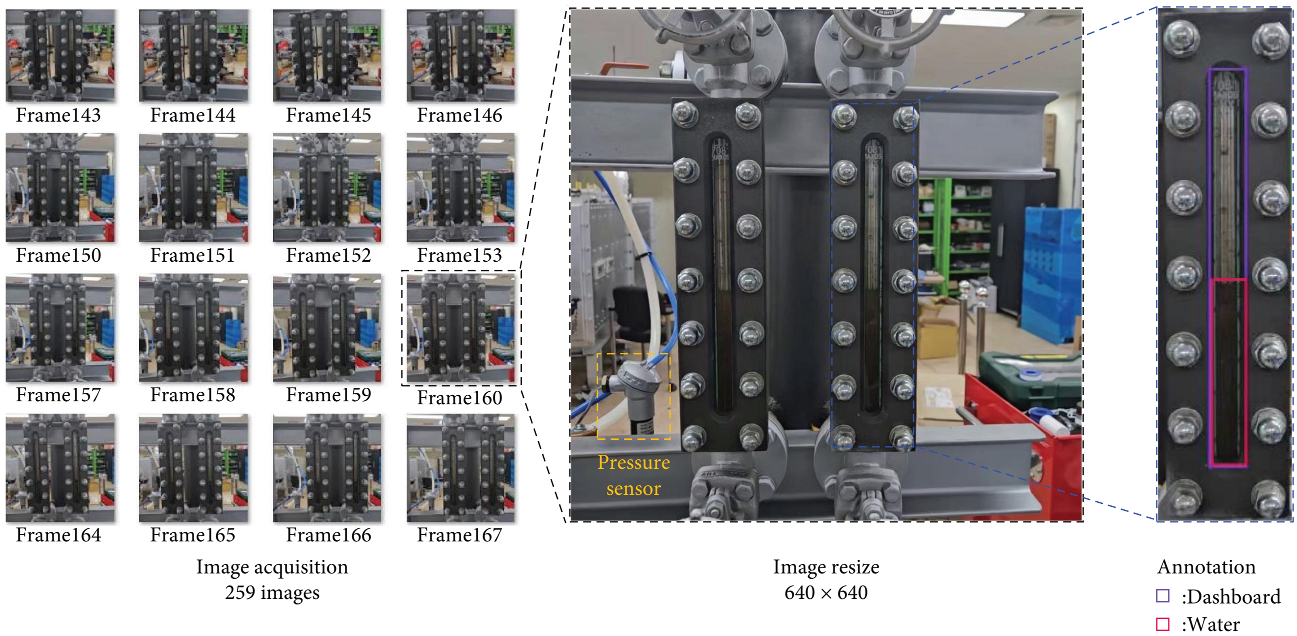

Figure 3: Creation of the training image dataset.

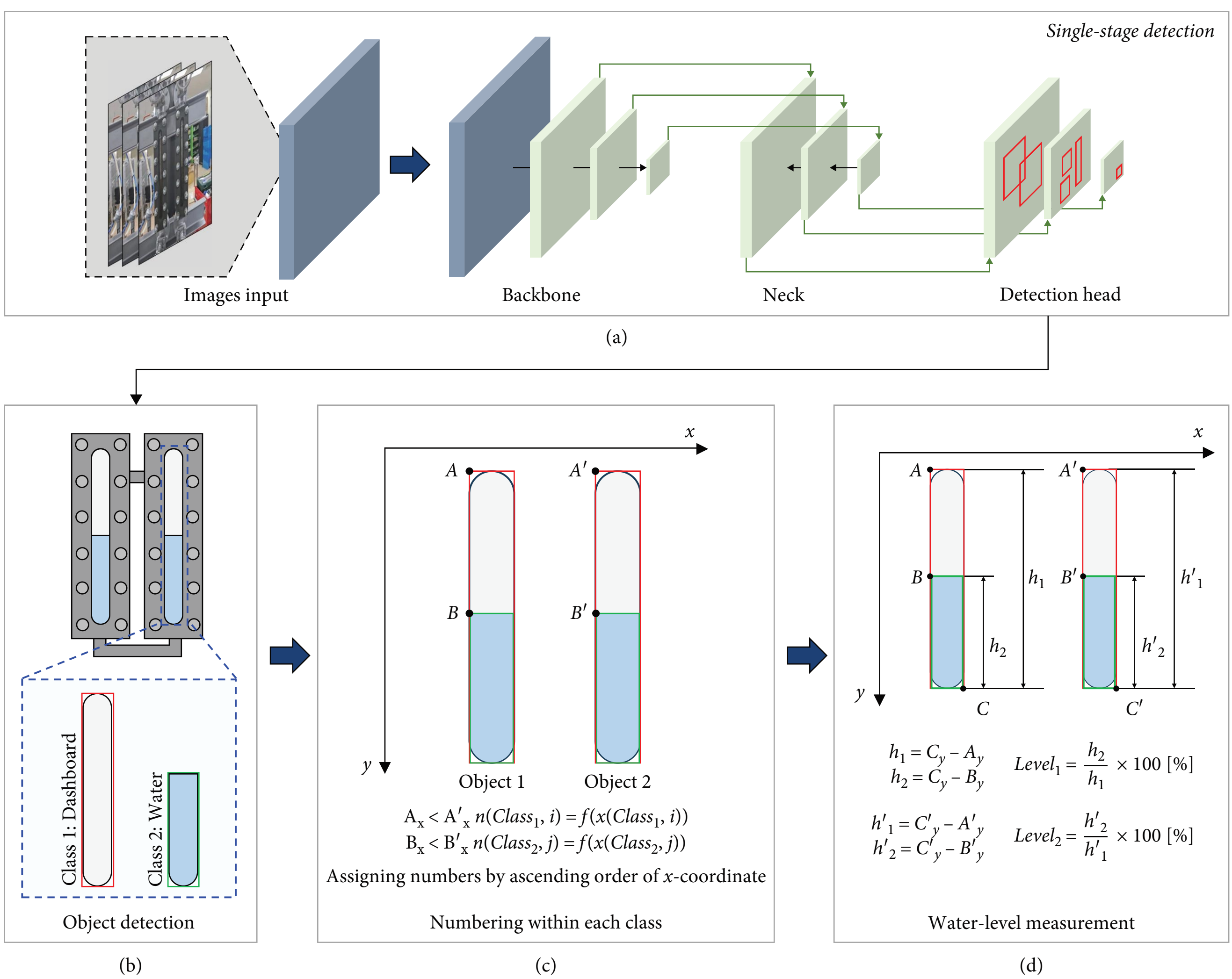

Figure 4: Schematics of the water-level measurement system based on the YOLOv5 algorithm: (a) architecture of the YOLOv5 algorithm, (b) object extraction and classification, (c) identification of each class, and (d) calculation of parameters for water-level measurement.

network of the model, extracting feature maps from the input images and capturing low-level features. The CSPDarknet53 network structure is used as the backbone for all YOLOv5 series models [20]. The neck combines features from the backbone to efficiently merge high-and low-level features, enhancing object detection performance for various scales. This enables the model to detect objects effectively, regardless of their size. Based on the feature maps processed by the neck, the head predicts the final positions (bounding boxes) of objects and their corresponding classes. YOLOv5 is a single-stage detector that efficiently detects objects of various sizes and shapes in a single step. It has different variants, such as YOLOv5x, v5l, v5m, v5s, and v5n, which are categorized by adjusting the network depth and width. Improved detection capabilities can be achieved by employing more complex networks. However, this comes with an increased demand for computer performance, resulting in longer training and detection response times. Therefore, selecting an appropriate model is crucial [14].

As shown in Figure 4(b), the trained model detects two classes in real-time water-level images: a dashboard (highlighted with red boxes) and water (highlighted with green boxes). The trained model ensured the consistent recognition of objects classified under the same class. The extracted objects needed to be distinguished to calculate the heights of the left and right water gauges separately. As shown in Figure 4(c), identification numbers were assigned based on the x-coordinates of the top-left corner of each bounding box. The heights of objects classified as classes 1 and 2 are represented by h_1 and h_2, respectively, with the numbering process assigning the number 1, as shown in Figure 4(d). Similarly, h'_1 and h'_2 represent the heights of the objects assigned the number 2 during the numbering process. The water levels were calculated as the height ratios of the bounding boxes, and percentage values were given as output. The average of the output water-level values can be converted into a 4–20 mA current signal, which is suitable for industrial control standards and can be used as an input signal for water pumps.

2.5. Model Performance Evaluation Metric. The proposed method for measuring water levels relies on the accuracy of the bounding boxes. Therefore, the optimal water-level detection model utilized the sum of the loss functions, as expressed in Equation (1).

$$\text{loss} = l_{\text{box}} + l_{\text{object}} + l_{\text{classification}}. \tag{1}$$

YOLOv5′s loss function includes bounding box loss (l_{box}), object loss (l_{object}), and classification loss ($l_{\text{classification}}$). These were used to evaluate the extent of disparity between the model's predictions and actual data. Additionally, during the training process, the loss of the training set (training loss) and the validation set (validation loss) were monitored to obtain the optimal detection model and prevent underfitting or overfitting.

In the context of computer vision, precision (pre) is defined as the ratio of the true predicted bounding box to all predicted bounding boxes. Similarly, recall (rec) is defined as the ratio of the true bounding box to all ground truths. These metrics assist in the evaluation of both the accuracy and completeness of the object detection model. Precision and recall were calculated using true positives (TP), false positives (FP), true negatives (TN), and false negatives (FN), as expressed in Equations (2) and (3).

$$\text{pre} = \frac{\text{TP}}{\text{TP} + \text{FP}}. \tag{2}$$

$$\text{rec} = \frac{\text{TP}}{\text{TP} + \text{FN}}. \tag{3}$$

The F1 score (F_1) represents the weighted average of precision and recall. It is calculated as the harmonic mean of the two values, and is therefore referred to as the harmonic mean of precision and recall, as expressed in Equation (4).

$$\text{F}_1 = \frac{2 \times \text{pre} \times \text{rec}}{\text{pre} + \text{rec}}. \tag{4}$$

Intersection over union (IoU) is a metric used in object detection models to measure the overlap between the predicted results and actual objects, as expressed in Equation (5).

$$\text{IoU} = \frac{\text{Intersection area}}{\text{Union area}}. \tag{5}$$

The mean average precision (mAP) reflects the overall detection performance of the model and is calculated as the mean value of each category's (c) area under the precision–recall curve, as expressed in Equations (6), and (7).

$$\text{AP} = \int_0^1 (\text{pre} \cdot \text{rec})\text{drec}. \tag{6}$$

$$\text{mAP} = \frac{1}{\text{C}} \sum_{\text{i}=1}^{\text{c}} \text{AP}_\text{i}. \tag{7}$$

The mAP was then calculated using IoU thresholds ranging from 0.5 (indicating partially accurate predictions) to 0.95 (indicating predictions that almost completely align with the ground truth). This measurement assessed the accuracy of the model in predicting objects at various levels of overlap with the ground truth.

3. Results

3.1. Training Results of the Object Recognition Model. The proposed method for measuring water levels involves calculating the direct ratio of bounding boxes. Therefore, the accuracy of the object detection model in classifying and detecting accurate positions through bounding boxes can directly affect water level detection. Figure 5 shows the training results for YOLOv5 models with various depths and widths. Each model was trained under the same conditions with 1,000 epochs, a batch size of 16, and an image size of 640.

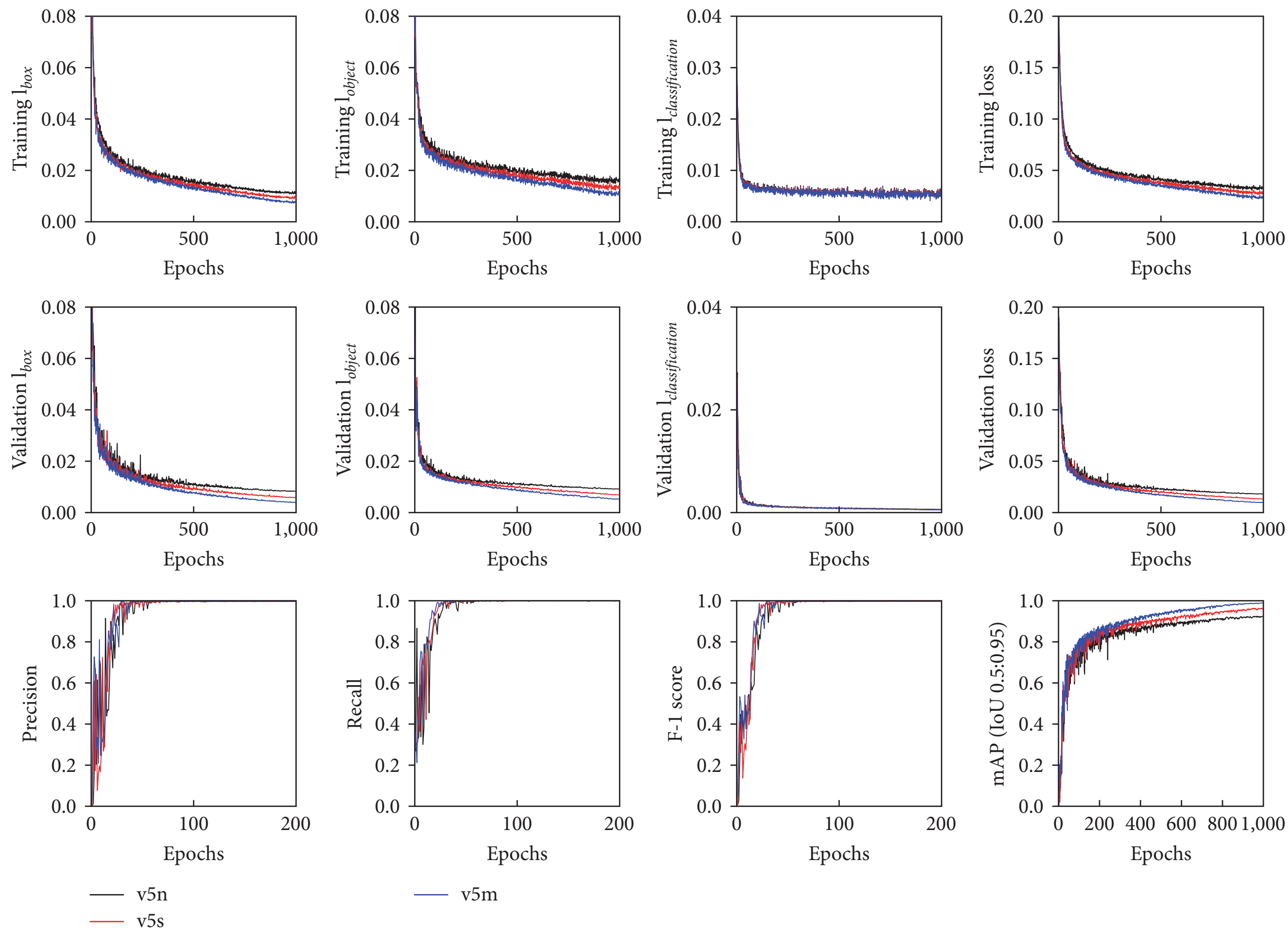

FIGURE 5: Training results for YOLOv5n, s, and m models on a custom dataset with 1,000 iterations.

TABLE 1: Performance differences of trained models.

Model	Layers	Parameter	Weights (kB)	Training time	Training loss	Validation loss	Response time (ms)		
							GPU	CPU	Rasp Pi 4B
YOLOv5n	157	1,761,871	3,823	2 hr 02 min	0.03110	0.01808	7.2	156.0	731.1
YOLOv5s	157	7,015,519	14,111	2 hr 48 min	0.02592	0.01327	7.9	428.3	1992.8
YOLOv5m	212	20,856,975	41,245	4 hr 13 min	0.02189	0.00968	14.3	1065.1	3749.2

Note. The training conditions for each model included 1,000 epochs, a batch size of 16, and an input size of 640. Training time varies depending on the performance of the server environment.

The comparison of the training and validation loss functions confirmed that the model did not suffer from overfitting. Furthermore, the classification accuracy of all three models tended to converge after approximately 50 epochs, while the accuracy and precision of the bounding boxes tended to converge after approximately 950 epochs. All models demonstrated satisfactory F1 scores and mAP, indicating their ability to accurately detect the objects required for water level detection in the input images. Additional training results for models n, s, and m are presented in Table 1. As the complexity of the model network structure increased, the object detection performance improved. The water level in industrial boilers did not change rapidly, resulting in short response times observed in the n, s, and m models measured in various environments. However, as the network complexity of the model increased, the training and water level detection response times also increased significantly. Therefore, a resource-intensive training environment is necessary.

3.2. Comparison of Water-Level Measurement Performance. Figure 6 presents the results of the water-level measurements using models with excellent learning performance to validate the measurement mechanism shown in Figure 4. To compare the measurement performances, as shown in Figure 6(a), videos were captured by repeatedly draining for 10 s and maintaining the water level for 30 s after filling the water gauge.

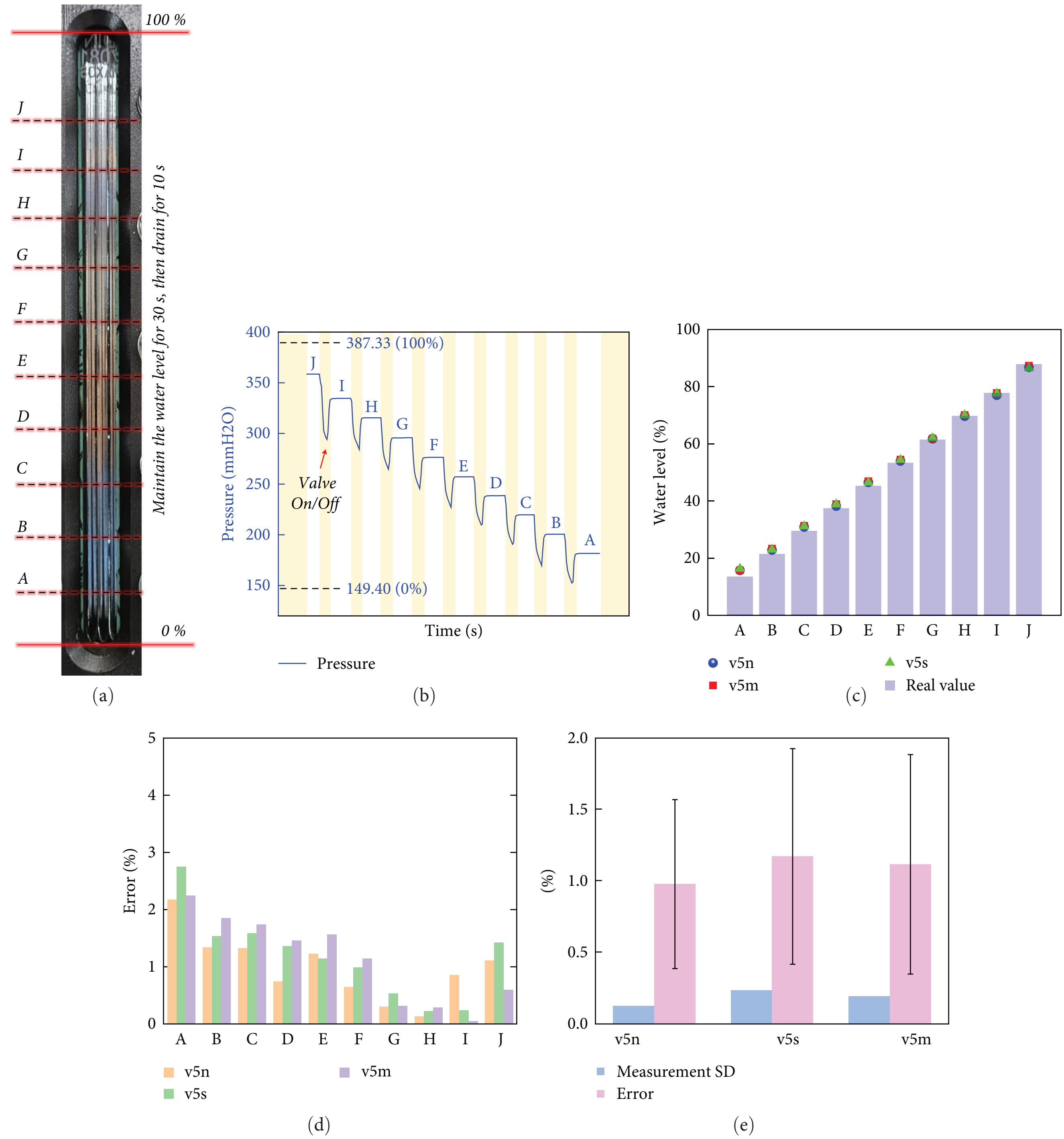

FIGURE 6: Performance of the model's water-level measurement: (a) lines for measuring water levels, (b) continuous pressure data measurements, (c) comparison of measurement data using the trained models, (d) comparison of segment-wise measurement errors for the models, and (e) comparison of standard deviation and mean error values of continuous water-level measurements for each model.

The video was captured from a location 40 cm away, maintaining a vertical angle to minimize the impact of the camera shooting angle on the water gauge. The actual values of each water-level line were extrapolated from the collected data through the pressure sensor, converted into ratios (0–100, unit: %)(149.40–387.33, unit: mmH_2O), as shown in Figure 6(b). The average water-level values for consistent lines A-J were obtained, excluding the section where interference occurred due to the pressure signal from the drainage valve. As shown in Figures 6(c) and 6(d), the recorded water-level states were continuously measured for each model, and the mean values of each model in each section were compared. All the models showed a trend of matching the actual water level across the entire section, with a minimum accuracy of 97.25% and a maximum of 99.47%.

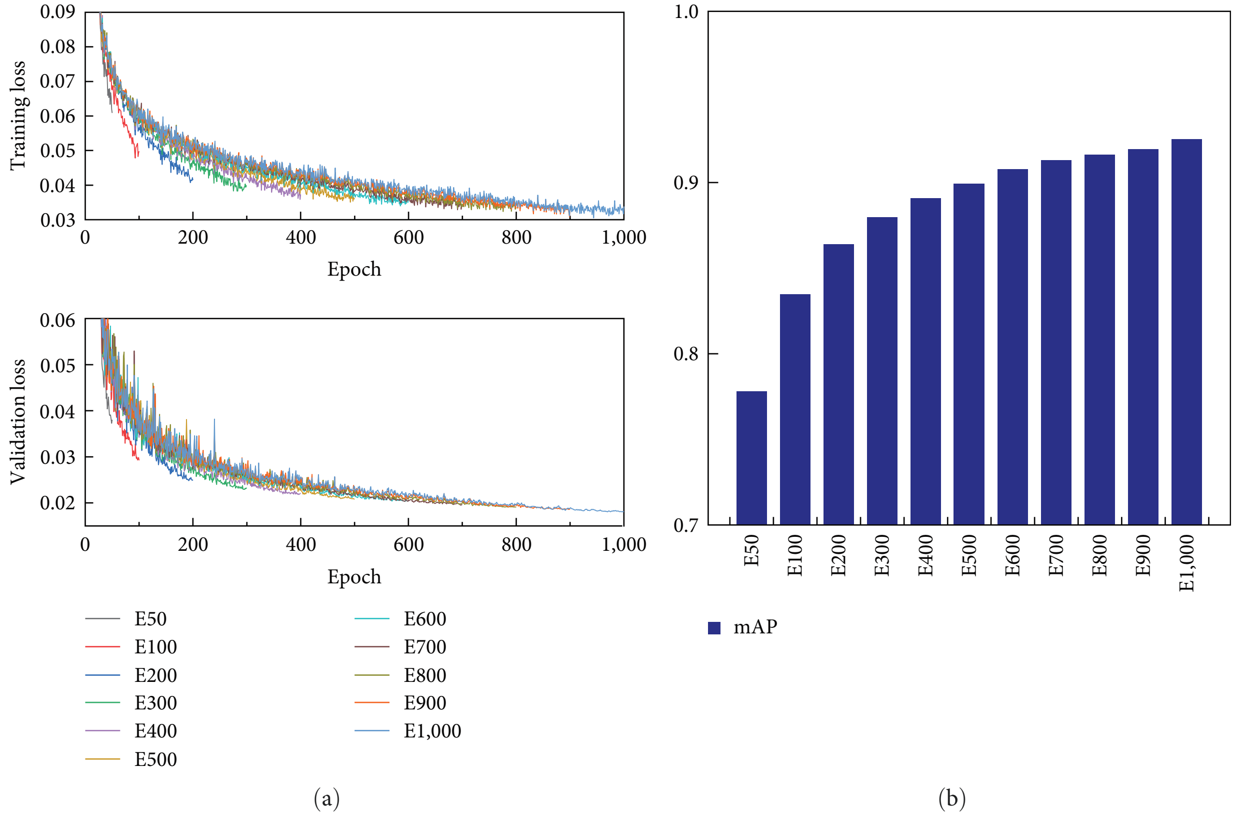

Figure 7: Performance metrics of models trained with varying numbers of iterations (E50-1000): (a) comparison of loss functions with respect to the number of iterations and (b) comparison of mAP with respect to the number of iterations.

However, accuracy tended to decrease in the edge regions of the water gauge. When measuring water levels in the field, it is crucial to consider the similarity between human vision and the camera and carefully plan camera placement.

Real-time object detection models exhibit a crucial characteristic of high variability in bounding boxes. This variability arises due to the adjustment of bounding box position and size frame-by-frame, creating the impression of fluctuation, even when the water level remains constant. Therefore, models with lower variability are better suited to obtaining stable water-level measurements. To evaluate the stability of water-level measurements for each model, the standard deviations of continuously collected measurement data at consistent water levels from A to J were compared, as shown in Figure 6(e). All three models performed well, with a bounding box variability of only 0.25%, indicating minimal impact on the measurements. The YOLOv5n model had the lowest variability. The YOLOv5n model exhibited the lowest variability. The average measurement error for the entire section was approximately 1%, indicating a high accuracy. Although the models had similar overall measurement performance, YOLOv5n exhibited the best performance for lightweight optimization when considering factors, such as weight, training time, and response time, as shown in Table 1.

3.3. Correlation between Detection Performance and Measurement Accuracy. As the number of training iterations increased, the object detection performance improved. However, with increasing training time and the accumulation of unnecessary training iterations, overfitting may occur. Furthermore, while the n, s, and m models showed outstanding object detection performance, this does not necessarily guarantee excellent water-level measurement performance. To compare the performance of water-level measurement based on the object recognition model's detection performance, iterative training was conducted using the "n" model, which exhibited the best water-level measurement performance with epoch sets ranging from 50 to 1,000. Subsequently, 11 trained models were used to measure the water level in a stable video recording water level (49.28%) for 10 s (Figure S1). Figure 7 illustrates the differences in detection performance based on the number of training iterations. The convergence of the loss function gradually decreased and the mAP improved as the number of training iterations increased (Figures 7(a) and 7(b)).However, although the enhanced detection performance was notable, there was no significant difference in accuracy and stability measurements in the stable water-level segment, as shown in Figure 8.

When establishing water-level conditions for feedback control in an industrial boiler, it is beneficial to select a range in which the signal remains stable and linear. To evaluate the efficacy of measurement techniques in fluctuating water-level environments, a series of experiments were conducted, wherein water was supplied at a consistent rate from 0% to 86.84%. The measurement performance for each model was evaluated using recorded water-level video (Figure S2). The results of the 328 sequences recorded over 10 s are shown in Figure 9. The sum of the readings was averaged to ensure uniform detection

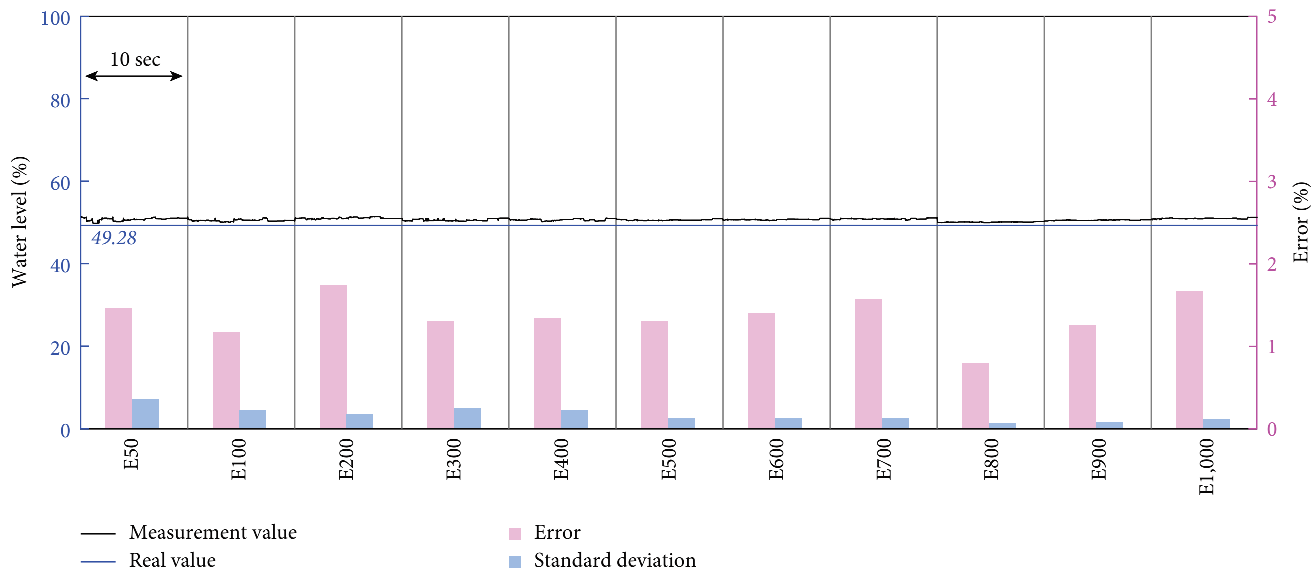

FIGURE 8: Comparison of the continuous measurement performance of models under steady water levels.

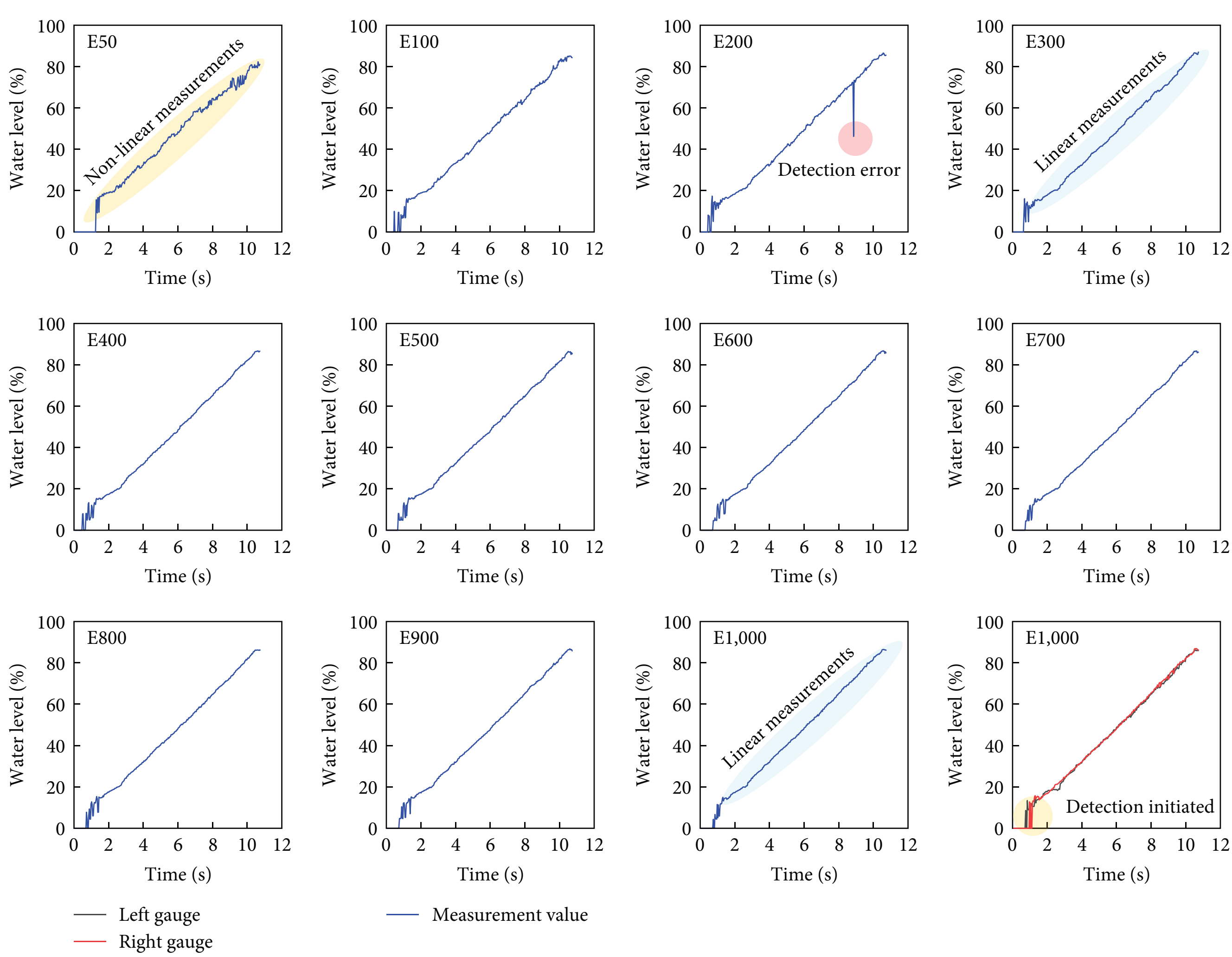

FIGURE 9: Comparison of continuous performance for different models under varying water-level conditions. The video length is 10 s, and the measurement values represent the average of the left and right gauge readings.

performance between the left and right gauges. The readings at E50, E100, and E200 show a nonlinear trend due to the difference in readings between the left and right gauges. This is a result of inaccurate bounding box generation due to insufficient model training iterations, where the model fails to accurately recognize learned class. Excluding the nonlinear output range caused by the time difference in the onset of detection between the left and right gauges when the "water" class starts to appear, the measurements at E300–E1000 showed a linear trend and their shapes were similar. Therefore, the loss function of E300 can be defined as a threshold that indicates linear measurement performance. As shown in Figure 7(a), models trained for over 300 iterations converge in terms of loss function values, and the linear range almost matches. These results show that the proposed measurement method is suitable for monitoring continuously changing water levels and maintaining constant water levels in industrial boilers.

Achieving stable measurement performance depends on achieving detection performance above a certain threshold through training, and setting an appropriate number of training iterations is crucial depending on the required accuracy. For example, water-level measurements aimed at ensuring safe operation may require lower accuracy and therefore fewer training iterations suitable for boiler operation. However, if the objective is to maintain a constant water level through feedback control, relatively more training iterations are required to reduce the variability and error. While it is possible to reduce the loss function by improving the quality of training data with more images and precise annotation, it is important to note that this may increase the costs associated with model development.

3.4. Advantages of Measurement Methods outside the Boiler System. The most prevalent capacitance measurement techniques [21] used in industrial settings are detailed in Table 2. These detection methods can be broadly categorized into contact-based and noncontact approaches. In the operation of industrial boilers, the drum pressure exceeds 80 bar [8], and the upper part of the boiler is filled with high-temperature steam. Consequently, sensors installed inside the drum to detect the liquid level noncontact are prone to signal interference, such as scattering and refraction [27]. Additionally, contact sensors struggle to continuously detect fluctuations in the drum's liquid level due to the boiling induced by the thermal energy from the furnace. The proposed method offers high measurement accuracy and stable performance (as illustrated in Figure 6), with the advantage of continuous quantification in both fluctuating and constant water-level conditions (as demonstrated in Figures 7 and 8). This distinguishes it from traditional sensors, as outlined in Table 2, in that the YOLO model-based measurement method can continuously quantify water levels from outside the boiler system without being affected by the harsh internal environment of the boiler.

4. Discussion

The YOLO-based object recognition technique used in this study is categorized as a single-stage detector, which is a type of object detection model that performs direct object localization and classification of input data simultaneously. It has been predominantly applied to tasks that prioritize real-time response times over accuracy, such as object identification [2, 3, 28] and the real-time tracking of fast-moving objects [29, 30].

However, this paper proposes a novel approach that utilizing bounding boxes generated during object detection with the YOLO algorithm to measure real-time water levels rapidly and accurately on a frame-by-frame basis. It was demonstrated that, when the detection targets and camera capturing the real-time video were fixed in position, the real-time changes in the objects could be measured quantitatively to a high degree. Furthermore, experiments showed that the variability in bounding boxes, potentially hindering water-level measurement stability, could be improved through iterative training and might not significantly affect measurement performance. This demonstrates the feasibility of overcoming the challenges of continuous variation measurements that require both rapid response times and high accuracy using the YOLO algorithm, which is a single-stage detector. As demonstrated in efforts to quantify water levels using cameras to maintain the infrastructure of industrial boilers, high-accessibility and low-development costs are essential for applying object recognition technology in the field. The costs paid for achieving better performance mainly include computational resources, such as CPU, GPU, or cloud computing instances, and the time spent on model training. Additional time may be necessary to acquire images for model training and to perform annotation tasks. Techniques such as hyperparameter tuning of the YOLO algorithm architecture or augmentation processing with more data may be necessary to achieve more precise detection performance. However, this study has shown that sufficient water-level measurement performance can be achieved with minimal processing, ensuring high accessibility for development. Limitations may arise in generalizing to all types of water gauges due to the technology's mechanism, which intuitively learns the form of the water gauge. Nevertheless, the high accessibility of development, facilitated by water gauge photos and open-source development tools, proves cost-effective and showcases the potential for customized development for different boilers.

The proposed system is composed of a small camera and an MCU, making it economically feasible and easily applicable to existing industrial boiler facilities without the need for modification or repair. This system allows obtaining water-level information not only as visual data but also in quantified form, with the advantage of the ease of utilizing various water-level measurement models by simply replacing the trained model file on the MCU. This flexibility enables the most suitable model to be used for measurements under different conditions.

Note that, similar to visual monitoring, errors can occur depending on the camera position when checking water levels. This can be addressed by flexibly adjusting the camera placement according to the requirements when applying the water-level measurement process in the field. The proposed method can be applied to other tasks that aim to quantify real-time changes in objects at fixed positions.

Table 2: Traditional methods for water-level measurement.

Type	Classification	Mechanism	Limitations	Application	Refs.
Pressure	Contact	The fluctuations in liquid pressure resulting from changes in liquid level are detected through the diaphragm.	Mainly usable in ranges close to atmospheric pressure. Measurements can be skewed in liquids with high gas content, and accuracy deteriorates if internal corrosion or sedimentation occurs.	Waste management, lake, river, vented tank and reservoir, etc.	[21, 22]
Differential pressure	Contact	Level is calculated by subtracting the tank pressure from the liquid pressure.	The presence of numerous air bubbles in the liquid results in inconsistent pressure, which in turn impairs the accuracy of the measurement. The outcome may vary depending on the attachment location.	Waste management, lake, river, vented tank and reservoir, etc.	[23]
Capacitive sensor	Contact	Probe electrodes suspended from the tank ceiling form a capacitor with the tank wall. As the measurement substance enters between the electrodes, the capacitance changes proportionally, which is measured and converted into a stored level.	Under changing temperature and pressure conditions, the dielectric constant of the water varies, leading to accuracy degradation due to capacitance differences caused by corrosion and sedimentation.	Part detection on work station, conveyors and robots, etc.	[24]
Float	Contact	Float is buoyed on the liquid surface, and the length to the float is monitored after accounting for variations in the liquid level.	Significant errors occur in point measurements due to fluctuations in the surface level.	Commercial, generator fuel, agriculture, etc.	[21]
Ultrasound	Noncontact	An ultrasonic pulse is emitted from the sensor, and the time taken for the pulse to reflect off the measurement material and return to the sensor is measured and converted into a value.	Temperature variations or the presence of gases within the measurement area can alter the speed of sound, leading to errors.	Fuel industries, manufacturing industries, etc.	[21]
Radar	Noncontact	Continuously vary the microwave frequency and emit it inside the tank. Measure the frequency difference between the emitted and reflected microwaves from the liquid inside the tank.	Involves complex numerical design and analysis. Requires additional design elements to lower the sensor operating temperature.	Chemical processing and water management, etc.	[21, 25]
Optical fiber	Noncontact	An optical fiber sensing probe is immersed in a liquid. The liquid-level is measured based on the reference emitted light, which is determined from the infrared light detected by the photodetectors.	The product is costly, with complex installation and operational procedures, and maintenance costs are relatively high.	Chemical and processing industries, etc.	[21, 26]

This study demonstrated the accuracy and measurement stability of the model by separating the water-level control part of the boiler at the laboratory scale. Future research will involve validating the utility of the developed model through field tests in actual industrial boilers. To improve learning performance and algorithm generalization, it may be necessary to expand the diversity of commercialized water gauges in image data. Furthermore, to minimize the impact of external factors in industrial systems, such as stains and lighting, expanding the training image set should be considered. The ultimate objective is to use water-level conditions as parameters for multidimensional deep learning analysis to improve boiler energy efficiency.

5. Conclusion

This study presents a method for quantitatively measuring the water-level state of a boiler drum in an existing industrial water-level control system. The method is based on the YOLO algorithm and utilizes the YOLOv5n model, which is suitable for low-spec environments. The model achieved an accuracy of 99.02% in water-level measurement. Despite the commonly known high variability of bounding boxes, the standard deviation of the measurement values remained at 0.13%, demonstrating excellent stability in continuous measurements. Additionally, the proposed water-level measurement algorithm exhibited robust real-time performance with fast response times averaging 7.2 ms on GPU, 156.0 ms on CPU, and 731.1 ms on Raspberry Pi. The proposed measurement system demonstrated an excellent performance without the need for text detection, proving its potential for efficiently improving complex boiler systems through object recognition technology and reliable water-level measurement and control.

Data Availability

The data that support the findings of this study are available from the corresponding author upon reasonable request

Conflicts of Interest

There are no conflicts of interest to declare.

Authors' Contributions

Jongwon Kim and Minjun Kwon contributed equally.

Acknowledgments

This work was supported by the Korea Institute of Energy Technology Evaluation and Planning (KETEP) and Ministry of Trade, Industry, and Energy (MOTIE) of the Republic of Korea (no. 20222020900040).

Supplementary Materials

Actual captured images showing the performance of different models under consistent water-level conditions (Figure S1) and varying water-level conditions (Figure S2). (*Supplementary Materials*)

References

[1] F. Meng, J. Li, Y. Zhang, S. Qi, and Y. Tang, "Transforming unmanned pineapple picking with spatio-temporal convolutional neural networks," *Computers and Electronics in Agriculture*, vol. 214, Article ID 108298, 2023.

[2] Y. Tian, G. Yang, Z. Wang, H. Wang, E. Li, and Z. Liang, "Apple detection during different growth stages in orchards using the improved YOLO-V3 model," *Computers and Electronics in Agriculture*, vol. 157, pp. 417–426, 2019.

[3] Z. Wang, L. Jin, S. Wang, and H. Xu, "Apple stem/calyx real-time recognition using YOLO-v5 algorithm for fruit automatic loading system," *Postharvest Biology and Technology*, vol. 185, Article ID 111808, 2022.

[4] K. Hu, Z. Chen, H. Kang, and Y. Tang, "3D vision technologies for a self-developed structural external crack damage recognition robot," *Automation in Construction*, vol. 159, Article ID 105262, 2024.

[5] H. Wang, X. Xu, Y. Liu, D. Lu, B. Liang, and Y. Tang, "Real-time defect detection for metal components: a fusion of enhanced canny–devernay and YOLOv6 algorithms," *Applied Sciences*, vol. 13, no. 12, Article ID 6898, 2023.

[6] Y. Tang, Z. Huang, Z. Chen et al., "Novel visual crack width measurement based on backbone double-scale features for improved detection automation," *Engineering Structures*, vol. 274, Article ID 115158, 2023.

[7] D. Zhao, F. Shao, Q. Liu, L. Yang, H. Zhang, and Z. Zhang, "A small object detection method for drone-captured images based on improved YOLOv7," *Remote Sensing*, vol. 16, no. 6, Article ID 1002, 2024.

[8] G. B. Raja, "Industrial boiler safety monitoring system," in *Industrial Control Systems*, pp. 15–36, Wiley, 2024.

[9] A. J. Abougarair, A. A. Amhathib, M. K. Elmezughi, and A. M. Almaktoof, "Supervisory control and simulation of boiler drum water level," in *2023 IEEE International Conference on Advanced Systems and Emergent Technologies (IC_ASET)*, pp. 1–6, IEEE, Hammamet, Tunisia, 2023.

[10] C. Cai, H. Meng, R. Qiao, and Q. Zhu, "Liquid-level measurement system based on second-confirm recognition algorithm," *Journal of Electronic Imaging*, vol. 27, no. 6, Article ID 063009, 2018.

[11] G. Chen, K. Bai, Z. Lin et al., "Method on water level ruler reading recognition based on image processing," *Signal, Image and Video Processing*, vol. 15, no. 1, pp. 33–41, 2021.

[12] G. Dou, R. Chen, C. Han, Z. Liu, and J. Liu, "Research on water-level recognition method based on image processing and convolutional neural networks," *Water*, vol. 14, no. 12, Article ID 1890, 2022.

[13] R. Qiu, Z. Cai, Z. Chang, S. Liu, and G. Tu, "A two-stage image process for water level recognition via dual-attention CornerNet and CTransformer," *The Visual Computer*, vol. 39, no. 7, pp. 2933–2952, 2023.

[14] G. Jocher, A. Chaurasia, A. Stoken et al., "ultralytics/yolov5: v7. 0-yolov5 sota realtime instance segmentation," Zenodo, 2022.

[15] Y. Dinesh, K. Ramalingam, P. Ramani, and R. M. Deepak, "Machine learning in the detection of oral lesions with clinical intraoral images," *Cureus*, vol. 15, no. 8, Article ID e44018, 2023.

[16] S. Dalal, B. Seth, M. Radulescu, T. F. Cilan, and L. Serbanescu, "Optimized deep learning with learning without forgetting (LwF) for weather classification for sustainable transportation and traffic safety," *Sustainability*, vol. 15, no. 7, Article ID 6070, 2023.

[17] A. A. Prisilla, Y. L. Guo, Y.-K. Jan et al., "An approach to the diagnosis of lumbar disc herniation using deep learning models," *Frontiers in Bioengineering and Biotechnology*, vol. 11, Article ID 1247112, 2023.

[18] E. Elhariri, N. El-Bendary, and S. M. Saleh, "Strawberry-DS: dataset of annotated strawberry fruits images with various developmental stages," *Data in Brief*, vol. 48, Article ID 109165, 2023.

[19] T.-H. Wu, T.-W. Wang, and Y.-Q. Liu, "Real-time vehicle and distance detection based on improved yolo v5 network," in *3rd World Symposium on Artificial Intelligence (WSAI)*, pp. 24–28, IEEE, Guangzhou, China, 2021.

[20] C.-Y. Wang, H.-Y. M. Liao, Y.-H. Wu, P.-Y. Chen, J.-W. Hsieh, and I.-H. Yeh, "CSPNet: a new backbone that can enhance learning capability of CNN," in *Proceedings of the IEEE/CVF conference on computer vision and pattern recognition workshops*, pp. 390-391, IEEE, 2020.

[21] P. Mohindru, "Development of liquid level measurement technology: a review," *Flow Measurement and Instrumentation*, vol. 89, Article ID 102295, 2023.

[22] M. Barzegar, S. Blanks, S. Gharehdash, and W. Timms, "Development of IOT-based low-cost MEMS pressure sensor for groundwater level monitoring," *Measurement Science and Technology*, vol. 34, no. 11, Article ID 115103, 2023.

[23] R. B. Mishra, N. El-Atab, A. M. Hussain, and M. M. Hussain, "Recent progress on flexible capacitive pressure sensors: from design and materials to applications," *Advanced Materials Technologies*, vol. 6, no. 4, Article ID 2001023, 2021.

[24] J. R. Hanni and S. K. Venkata, "A novel helical electrode type capacitance level sensor for liquid level measurement," *Sensors and Actuators A: Physical*, vol. 315, Article ID 112283, 2020.

[25] B. T. Sivaprakasam, C. V. Krishnamurthy, and K. Arunachalam, "Design and demonstration of a RADAR gauge for in-situ level measurement in furnace," *IEEE Sensors Journal*, vol. 18, no. 10, pp. 4081–4088, 2018.

[26] C. Dalai, M. Singh, A. S. Kumara, W. Patel, H. Patil, and R. Maranan, "Monitoring water levels in rivers with optical fiber sensors," in *5th International Conference on Innovative Trends in Information Technology (ICITIIT)*, pp. 1–6, IEEE, Kottayam, India, 2024.

[27] P. Mikuš, R. Harťanský, and O. Čičáková, "Diffraction problem in radar level gauge verification," *Universal Journal of Electrical and Electronic Engineering*, vol. 2, no. 4, pp. 165–169, 2014.

[28] C. Zhang, C.-C. Chang, and M. Jamshidi, "Concrete bridge surface damage detection using a single-stage detector," *Computer-Aided Civil and Infrastructure Engineering*, vol. 35, no. 4, pp. 389–409, 2020.

[29] Y. Wageeh, H. E.-D. Mohamed, A. Fadl et al., "YOLO fish detection with Euclidean tracking in fish farms," *Journal of Ambient Intelligence and Humanized Computing*, vol. 12, no. 1, pp. 5–12, 2021.

[30] M. Simon, K. Amende, A. Kraus et al., "Complexer-yolo: real-time 3d object detection and tracking on semantic point clouds," in *Proceedings of the IEEE/CVF Conference on Computer Vision and Pattern Recognition Workshops*, IEEE, 2019.